

The ${}^2\text{H}(\alpha, \gamma){}^6\text{Li}$ experiment at LUNA

Carlo Gustavino^{1,a} for the LUNA Collaboration

¹Dipartimento di Fisica, Università di Roma and INFN, Sezione di Roma1, I-00185, Rome, Italy

Abstract. Recent observations of ${}^6\text{Li}$ in metal poor stars suggests a huge production of this isotope during BBN, through the ${}^2\text{H}(\alpha, \gamma){}^6\text{Li}$ reaction. This reaction has never been directly measured inside the BBN energy region because its cross section drops steeply at low energy, while indirect measurements using the Coulomb dissociation of ${}^6\text{Li}$ only give upper limits due to the dominance of nuclear breakup process. Exploiting the ultra-low background at the 400 keV LUNA accelerator, located deep underground in Italy's Gran Sasso laboratory, for the first time the reaction has been measured directly at BBN energy. The LUNA data and their implications for the BBN theory are discussed.

1 Introduction

In its standard picture, the Big Bang Nucleosynthesis occurs during the first minutes of universe, with the formation of light isotopes such as D , ${}^3\text{He}$, ${}^4\text{He}$, ${}^6\text{Li}$ and ${}^7\text{Li}$. Their abundance only depends on standard model physics, on the baryon-to-photon ratio η and on the nuclear cross sections of involved processes. The observations of D , ${}^3\text{He}$, and ${}^4\text{He}$ abundances are in good agreement with calculations, confirming the overall validity of BBN theory. On the other hand, the observed abundance of ${}^7\text{Li}$ is a factor 2-4 lower than the predicted one, while the amount of ${}^6\text{Li}$ observed in metal poor stars is unexpectedly large compared to Big Bang Nucleosynthesis (BBN) predictions, about 3 orders of magnitude higher than the calculated value [1]. Even though many of the claimed ${}^6\text{Li}$ detections are controversial, for a few metal-poor stars there still seems to be a significant amount of ${}^6\text{Li}$ [1]. The difference between observed and calculated abundances of ${}^7\text{Li}$ and ${}^6\text{Li}$ may reflect unknown post-primordial processes or physics beyond the Standard Model, and are reported in literature as the "*Primordial Lithium problems*" [1, 2]. In standard BBN, the leading process to synthesize ${}^6\text{Li}$ is the ${}^2\text{H}(\alpha, \gamma){}^6\text{Li}$ reaction. The ${}^2\text{H}(\alpha, \gamma){}^6\text{Li}$ cross section is very small at BBN energies ($30 \lesssim E(\text{keV}) \lesssim 400$), because of the Coulomb barrier and because electric dipole transition is suppressed for the iso-scalar particles ${}^2\text{H}$ and ${}^4\text{He}$ [3]. Therefore, the ${}^2\text{H}(\alpha, \gamma){}^6\text{Li}$ cross section has been measured only for energies greater than 1 MeV and around the 711 keV resonance [4, 5]. There are two indirect attempts to determine the ${}^2\text{H}(\alpha, \gamma){}^6\text{Li}$ cross section at BBN energies, using the Coulomb dissociation technique [6, 7]. In this approach, the time-reversed reaction ${}^6\text{Li}(\gamma, \alpha){}^2\text{H}$ is studied using an energetic ${}^6\text{Li}$ beam and a target of high nuclear charge. However, it is difficult to unfold the cross section with this method, because the nuclear effects are dominant and the result strongly depends on the theoretical assumptions [3, 7]. The present work reports on the first direct measurement of the ${}^2\text{H}(\alpha, \gamma){}^6\text{Li}$ at BBN energies, performed by

^ae-mail: carlo.gustavino@roma1.infn.it

the LUNA collaboration (LUNA=Laboratory for Underground Nuclear Astrophysics). The measurement has been carried with the world only underground accelerator, situated at the LNGS laboratory (LNGS=Laboratorio Nazionale del Gran Sasso), Italy [8]. The "Gran Sasso" mountain provides a natural shielding which reduces the muon and neutron fluxes by a factor 10^6 and 10^3 , respectively. The suppression of the cosmic ray induced background also allows an effective suppression of the γ -ray activity by a factor 10^2 - 10^5 , depending on the photon energy [9]. The ultra-low background at LNGS made possible to study the ${}^2\text{H}(\alpha, \gamma){}^6\text{Li}$ reaction at Big Bang energies. In the following, the new data and their implications for Big Bang nucleosynthesis will be shown.

2 Measurement

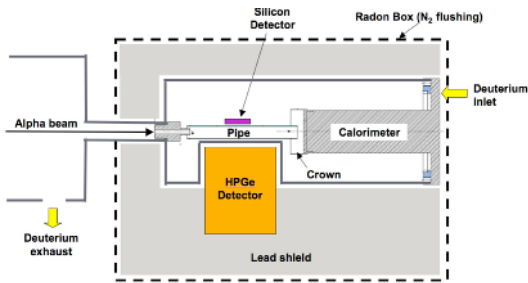


Figure 1. (Colour online) Sketch of experimental set-up.

Fig. 1 shows the experimental set-up used for the ${}^2\text{H}(\alpha, \gamma){}^6\text{Li}$ reaction. The measurement is based on the use of the 400 kV accelerator, that provides an α -beam of high intensity. The α -beam impinges a windowless gas target of D_2 , with a nominal operating pressure of 0.3 mbar. The signal is maximized by stretching the beam intensity up to about 350 μA and by using a configuration with the high purity Ge(Li) detector (HPGe) as close as possible to the beam line. The natural background of LNGS is further reduced by means of a 4π lead shield around the reaction chamber and the HPGe detector. The set-up is enclosed in a anti-radon box flushed with high purity N_2 , to reduce and stabilize the γ activity due to the radon decay chain. The measurement of the ${}^2\text{H}(\alpha, \gamma){}^6\text{Li}$ reaction is affected by an inevitable beam induced background. In fact, the ${}^2\text{H}(\alpha, \alpha){}^2\text{H}$ Rutherford scattering induces a small amount of ${}^2\text{H}({}^2\text{H}, n){}^3\text{He}$ ($Q = 3.267$ MeV) and ${}^2\text{H}({}^2\text{H}, p){}^3\text{H}$ ($Q = 4.033$ MeV) reactions. While the ${}^2\text{H}({}^2\text{H}, p){}^3\text{H}$ reaction is not a problem in this context, the neutrons produced by the ${}^2\text{H}({}^2\text{H}, n){}^3\text{He}$ reaction induce $(n, n'\gamma)$ reactions in the HPGe detector and in the surrounding materials (lead, steel, copper), generating a neutron induced background (here and after NIB) in the HPGe spectrum. To reduce the effective path for the scattered deuterons, and therefore the yield of the ${}^2\text{H}({}^2\text{H}, n){}^3\text{He}$ reaction, a removable 177 mm long tube, with a square cross section of 17×17 mm, is placed along the beam line (see Fig. 1). In this way, the neutron production is limited at the level of few neutrons/second. The set-up is implemented with a silicon detector faced to the gas target volume, to monitor the running conditions through the detection of protons generated in the ${}^2\text{H}({}^2\text{H}, p){}^3\text{H}$ reaction ($E_p \cong 3$ MeV). As a matter of fact, the proton rate is related to the number of produced neutrons, since the cross sections of the two conjugate ${}^2\text{H}({}^2\text{H}, n){}^3\text{He}$ and ${}^2\text{H}({}^2\text{H}, p){}^3\text{H}$ reactions are similar and well known [10]. Further details on the set-up can be found in [11].

The HPGe spectrum has three components: the natural background (BCK), the neutron induced background (NIB) and the signal due to the γ -rays produced in the ${}^2\text{H}(\alpha, \gamma){}^6\text{Li}$ reaction. To extract the signal due to the ${}^2\text{H}(\alpha, \gamma){}^6\text{Li}$ reaction it is therefore necessary to subtract BCK and NIB. The BCK is stable and low due to the lead shielding and the anti-radon box. Therefore, it has been measured separately in long off-beam measurements and properly subtracted. The NIB spectrum at LUNA

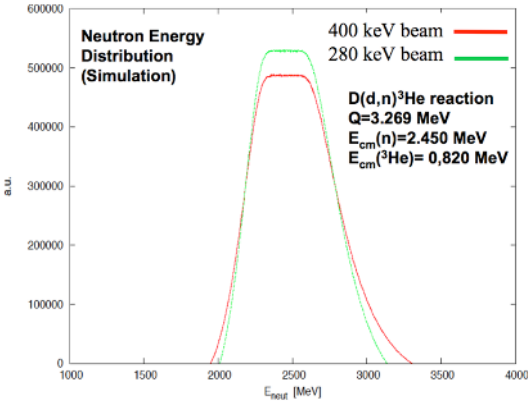


Figure 2. (Colour online) Energy distribution of neutrons produced by the ${}^2\text{H}({}^2\text{H}, n){}^3\text{H}$ reaction with $E_\alpha = 400 \text{ keV}$ (red line) and $E_\alpha = 280 \text{ keV}$ (green line), as obtained in the GEANT4 simulation [11].

has been extensively studied by means of experimental data and a detailed simulation based on the GEANT4 package [11]. Fig. 2 shows the energy distribution of neutrons at $E_{beam} = 400, 280 \text{ keV}$. It is worth to point out that the neutron energy distribution depends weakly on the beam energy, because the difference between the two beam energies $\Delta E_{beam} = 120 \text{ keV}$ is much smaller with respect to energy of neutrons produced in the ${}^2\text{H}({}^2\text{H}, n){}^3\text{H}$ reaction ($E_n = 2450 \text{ keV}$ in the center-of-mass system). As a consequence, the NIB shape is almost unaffected while changing the α -beam energy, because it is generated by the neutron interaction with the material surrounding the HPGe detector [11]. The energy of γ -rays produced by the ${}^2\text{H}(\alpha, \gamma){}^6\text{Li}$ reaction ($Q = 1473.48 \text{ keV}$) depends on kinematics through the following relationship:

$$E_\gamma = Q + E_{beam} \frac{m_D}{m_D + m_\alpha} \pm \Delta E_{doppler} - E_{recoil}(1)$$

In this equation, m_D and m_α are the masses of deuteron and α particles, respectively. In our set-up The Doppler correction is $\Delta E_{doppler} \approx 16 \text{ keV}$ at $E_\alpha = 400 \text{ keV}$, and the γ -ray energy shift due to the recoiling compound nucleus is about $E_{recoil} = 0.2 \text{ keV}$. As the γ -rays produced in the ${}^2\text{H}(\alpha, \gamma){}^6\text{Li}$ reaction depends on the beam energy, the NIB can be subtracted performing in-beam measurements at two different energies, that is:

1. Measurements with $E_{beam} = 400 \text{ keV}$ on D_2 target. The Ge spectrum is mainly due to the back-ground induced by neutrons. The ${}^2\text{H}(\alpha, \gamma){}^6\text{Li}$ γ signal is kinematically constrained in a well defined region of interest (RoI), $1587 < E_\gamma(\text{keV}) < 1625$.
2. Same as 1., but with $E_{beam} = 280 \text{ keV}$. In this case, the RoI of γ -rays produced in the ${}^2\text{H}(\alpha, \gamma){}^6\text{Li}$ reaction is shifted to the $1550 - 1580 \text{ keV}$ region.

As the RoIs of these two measurements do not overlap, the signal at 400 (280) keV can be extracted by subtracting the NIB obtained in the 280 (400) keV measurement. The in-beam measurements have been performed by alternating the two energies during the ~ 40 days of acquisition time (about 20 days for each beam energy). It has been found that the NIB rate is not related in a simple way to the working parameters such as the beam energy, beam intensity and target density. In fact, it slightly increases with time because of the progressive implantation of scattered deuterium in the material surrounding the beam line, such as the 177 mm long tube coaxial to the beam line (see fig. 1). As a consequence, the scattered deuterons interact not only with the deuterium gas target but also with the implanted deuterons, making the NIB rate dependent on the operation time. Therefore, the NIB_{280} has been normalized to the NIB_{400} one with a minimization procedure, leaving the normalization factor as a free parameter. Fig. 3 shows the spectra obtained with nominal beam energies of $E_\alpha = 400, 280 \text{ keV}$,

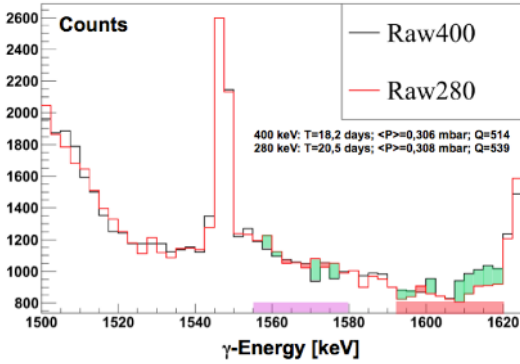


Figure 3. (Colour online) Experimental spectra for $E_\alpha = 400 \text{ keV}$ (black line) and for $E_\alpha = 280 \text{ keV}$ (red line). The natural background has been subtracted. The narrow peaks at 1547 keV and 1623.5 keV are due to the de-excitation of ^{63}Cu and ^{65}Cu isotopes induced by inelastic neutron scattering [11]. The red and violet bands indicate the RoI at $E_\alpha = 400 \text{ keV}$ RoI and $E_\alpha = 280 \text{ keV}$, respectively. Note the counting excesses visible (green bins) in correspondence to the RoIs.

respectively (*BCK* subtracted). The spectrum at $E_\alpha = 280 \text{ keV}$ have been normalized accordingly with the minimization procedure. The counting excess due to the $^2\text{H}(\alpha, \gamma)^6\text{Li}$ reaction is clearly visible in the $E_\alpha = 400 \text{ keV}$ RoI. The shape of the counting excess suggests a forward-backward asymmetry of emitted photons, possibly due to the interference between dipole and quadrupole transitions [3]. The reaction yield at $E_\alpha = 280 \text{ keV}$ is slightly lower with respect the one obtained at $E_\alpha = 400 \text{ keV}$, as a consequence of the higher Coulomb barrier and the absence of resonant nuclear effects. In the low energy domain, the cross section $\sigma(E)$ can be expressed using the astrophysical factor $S(E)$, defined by the formula:

$$\sigma(E) = \frac{S(E)e^{-2\pi\eta}}{E} \quad (2)$$

$S(E)$ contains all the nuclear effects and, for non-resonant reactions, it is a smoothly varying function of energy. The exponential term takes into account the Coulomb barrier. The Sommerfeld parameter η is given by $2\pi\eta = 31.29Z_1Z_2(\mu/E)^{1/2}$. Z_1 and Z_2 are the nuclear charges of the interacting nuclei. μ is their reduced mass (in units of a.m.u.), and E is the center of mass energy (in units of keV).

Fig. 4 shows the preliminar S_{24} astrophysical factor obtained by LUNA as a function of the center-of-mass energy, together with all previous direct measurements [4, 5]. As shown in the figure, the S_{24} astrophysical factor measured by LUNA is slightly in agreement with the theoretical S_{24} factors describing the Coulomb dissociation measurement by [7].

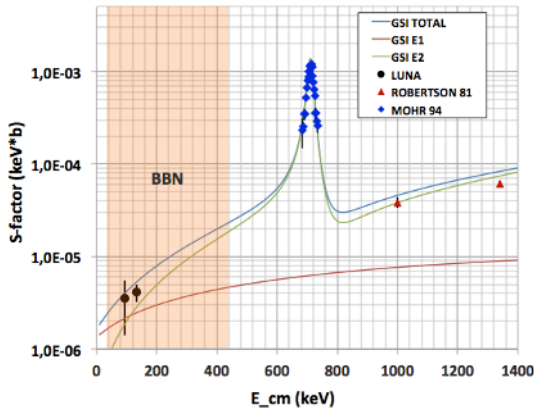


Figure 4. (Colour online) The astrophysical factor of the $^2\text{H}(\alpha, \gamma)^6\text{Li}$ reaction as a function of the center-of-mass energy. The preliminar result of the LUNA measurement (statistical error only) is shown with all the previous direct [4, 5] measurements. The continuous lines show the theoretical $E1$, $E2$, and total S_{24} factors describing the Coulomb dissociation measurement by [7]. The BBN energy of interest (orange band) is also shown.

3 Conclusions

The LUNA experiment provides the first direct measurement of the ${}^2\text{H}(\alpha, \gamma){}^6\text{Li}$ reaction inside the BBN region of interest, giving a robust experimental footing to compute the ${}^6\text{Li}$ primordial abundance. The LUNA data show that a nuclear solution to explain a huge abundance of primordial ${}^6\text{Li}$ in metal-poor stars is strongly disfavored, in agreement with previous indirect measurements and theoretical calculation. In fact, although the whole BBN energy of interest has not been investigated by LUNA, the existence of major nuclear effects such as an intense resonance at BBN energies is very unlikely, as it is excluded by the absence of nuclear levels below the quadrupole 711 keV resonance of ${}^6\text{Li}$. Concerning direct observations of ${}^6\text{Li}$, it has been argued that the convective motions on the stellar surface may give an asymmetry of the Li absorption line, thus mimicking the presence of a large amount of ${}^6\text{Li}$ in metal-poor stars [1]. For this reason the ${}^6\text{Li}$ observations remain controversial, although there is widespread agreement that ${}^6\text{Li}$ has even been detected on a few halo stars [1, 2]. On the other hand, the efficient production after BBN of the fragile ${}^6\text{Li}$ isotope looks very unlikely. Finally, assuming that direct observations of ${}^6\text{Li}$ reflect unexpected high production of this isotope during BBN, and that the nuclear physics of BBN holds no surprises, many authors suggest that the abundance of Lithium isotopes may be haltered by non-standard physics, such as annihilation/decay of super-symmetric particles or long lived, negatively charged massive particles [12-19]. In this concern, the BBN theory represent a powerful tool to investigate physics beyond the standard model, as far as the knowledge of relevant nuclear processes and all the other ingredients of standard BBN is accurate enough.

References

- [1] See proceedings of "Lithium in the Cosmos", 27-29 February 2012, Paris.
- [2] B.D. Fields, *Annu. Rev. Nucl. Part. Sci.* 61, 47 (2011).
- [3] L. Marcucci, K. Nollett, R. Schiavilla, and R. Wiringa, *Nucl. Phys. A* 777, 111 (2006).
- [4] R. G. H. Robertson et al., *Phys. Rev. Lett.* 47, 1867 (1981).
- [5] P. Mohr et al., *Phys. Rev. C* 50, 1543 (1994).
- [6] J. Kiener et al., *Phys. Rev. C* 44, 2195 (1991).
- [7] F. Hammache et al., *Phys. Rev. C* 82, 065803, 1011.6179 (2010).
- [8] A. Formicola et al., *Nucl. Instr. and Meth. A* 507, 609 (2003).
- [9] A. Caciolli et al., *Eur. Phys. J. A* 39, 179 - 186 (2009).
- [10] D.S. Leonard et al. *Phys. Rev. C* 73 045801 (2006).
- [11] M. Anders et al., *Eur. Phys. J. A* 49: 28 (2013).
- [12] R.H. Cyburt, et al. *J. Cosmol. Astropart. Phys.* 10:32 (2010).
- [13] K. Jedamzik, K. Choi, L. Roszkowski L, R. Ruiz de Austri, *J. Cosmol. Astropart. Phys.* 7:7 (2006).
- [14] M. Kusakabe et al., *Phys. Rev. D* 76:121302 (2007).
- [15] M. Pospelov, J. Pradler, F.D. Steffen, *J. Cosmol. Astropart. Phys.* 11:20 (2008).
- [16] K. Jedamzik, *Phys. Rev. D* 77:063524 (2008).
- [17] S. Bailly, K. Jedamzik, G. Moulataka, *Phys. Rev. D* 80:063509 (2009).
- [18] K. Jedamzik and M. Pospelov, *New Journal of Physics* 11, 105028 (2009).
- [19] M. Pospelov and J. Pradler, *Ann. Rev. Nucl. Part. Sci.* 60, 539 (2010).

